

Pin-supported Walls for Enhancing the Seismic Performance of Building Structures

Zhe Qu, Akira Wada, Shojiro Motoyui, Hiroyasu Sakata, and Shoichi Kishiki

Abstract: An application of a pin-supported wall-frame system in retrofitting an 11-story steel reinforced concrete frame is introduced. The retrofit aims at enhancing integrity and avoiding weak story failure in an existing moment-resisting frame. Seismic performance of the building before and after the retrofit is assessed through nonlinear dynamic analysis. The results show that the pin-supported walls are effective in controlling the deformation pattern of the ductile frame and hence in avoiding weak story failure. With the well-controlled deformation pattern, carefully arranged energy dissipating devices are able to concentrate energy dissipations so that damage to the rest of the structure can be significantly reduced.

Keywords: moment-resisting frame, pin-supported wall, integrity, steel damper, dual system

1 Introduction

Strength has long been recognized as the most important property of structures in resisting various types of external actions including earthquakes. With the advent of ductile moment-resisting frames in the 1950s, ductility was considered another essential property for structures to survive strong earthquakes. Energy dissipation capacity, which is directly dependent on ductility in a ductile moment-resisting frame, is believed very helpful in reducing seismic responses. Furthermore, ductility permits individual members or parts of a structure to collaborate so that the strength of the whole structure can be better developed. Moreover, proper control of the plastic mechanism of a structural system is also very important because it is closely related to the ductility demands for the different components of a structure.

Subjected to combined shear force, which is an idealization of horizontal earthquake actions (Figure 1(a)), a moment-resisting frame may develop various plastic mechanisms. Compared with the local ones (e.g., the column mechanism in Figure 1(b)), the global mechanism in Figure 1(c) is generally preferred because the strength and ductility of more structural components can contribute to resist the earthquake action. There is generally not adequate global component for the height of the structure and the column mechanism is thus not easy to avoid. This could also be attributed to a lack of integrity in the sense that individual stories or substructures in a system do not collaborate well. This has long been a problem. Many historic major earthquakes, e.g., the 1985 Mexico City earthquake and the 1995 Kobe earthquake, have seen the failure of many reinforced concrete frames in this kind of local mechanism [1, 2]. This has continued to be a problem. Weak story collapses of ductile reinforced concrete frames were observed in the 2008 M8.0 Wenchuan earthquake [3] and also in the most recent M9.0 Tohoku earthquake [4].

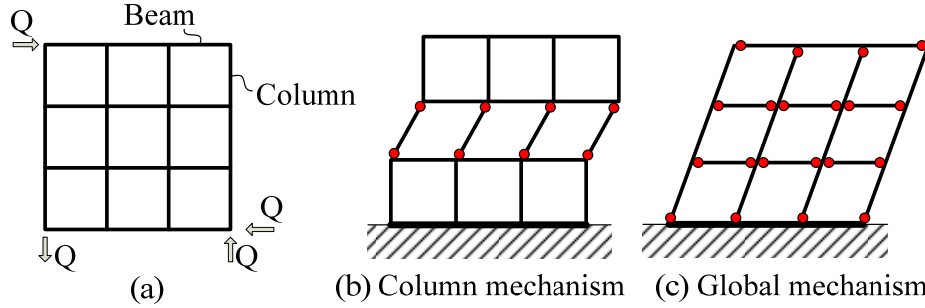


Figure 1 Possible plastic mechanisms of a moment-resisting frame under combined shear forces (Solid circles represent plastic hinges)

Various efforts have been devoted to enhancing the story-by-story integrity of ductile frames to avoid a weak story mechanism. The most widely accepted method is generally referred to as the “strong column-weak beam” criterion, which was proposed and discussed extensively by [Paulay and Priestley \[5\]](#). It has been stipulated in major seismic codes in the world for decades [6, 7, 8]. Some factors are applied to amplify the flexural strength demands for columns so that the total flexural strength of the columns framing into a joint is greater than that of the beams framing into the same joint.

Other researchers have focused on the effect of vertical continuous stiffness in mitigating damage concentration along the height of a structure. [Akiyama \[9, 10\]](#) investigated the relationship of damage concentration and the stiffness k_{eq} of the so-called “spreader column.” The basic model used is shown in [Figure 2\(a\)](#), where k_R is the story stiffness of the frame. The spreader column is connected to the frame and the foundation by hinges. The degree of damage concentration is expressed by the ratio of the damage index of the most heavily damaged story to that of the global structure. Equations to relate the degree of damage concentration and the stiffness ratio k_{eq}/k_R have been proposed based on time history analysis results with the 1940 El Centro NS and 1968 Hachinohe EW ground motion records.

A similar idea was applied by [MacRae et al. \[11\]](#) in steel concentrically braced frames with continuous columns, as shown in [Figure 2\(b\)](#). The continuous columns may be seismic or gravity columns, which are modeled as pinned at the base. The reduction of story drift concentration due to increasing flexural stiffness of continuous columns was examined through both static and dynamic nonlinear time history analysis. This issue was also examined by [Ji et al. \[12\]](#) but in a more analytical manner. [Tagawa \[13\]](#) extended this effort to moment-resisting steel frames.

Walls, usually with much larger and especially deeper cross sections, are much more effective than individual columns for providing flexural stiffness to control story drift. As pointed out by [Paulay and Priestley \[14\]](#), development of a weak story mechanism can readily be avoided as a result of the considerable stiffness of walls. In examining the effect of foundation flexibility on the seismic performance of a shear wall-frame dual system, they demonstrated the drift control effect and force distribution characteristics of dual systems with pinned base walls. The results of their nonlinear dynamic analysis indicate that loss of wall base restraint would not significantly impair the seismic performance of wall-frame systems.

[Alavi and Krawinkler \[15\]](#) proposed using walls to improve the seismic performance of frame structures subjected to near-fault ground motions. 20-story generic frame models were

built and dynamic nonlinear analysis was performed with an equivalent pulse motion as a representation of near-fault ground motions. The performance of hinged walls, as shown in Figure 2(c), was compared with that of conventional fixed-base shear walls. It was found that the strengthening of frame structures with hinged walls is effective in reducing the maximum story drift demands and producing a more uniform distribution of story drifts over the height of the structure. Moreover, the shear and moment demands for a hinged wall are much lower than are those for a fixed-base wall.

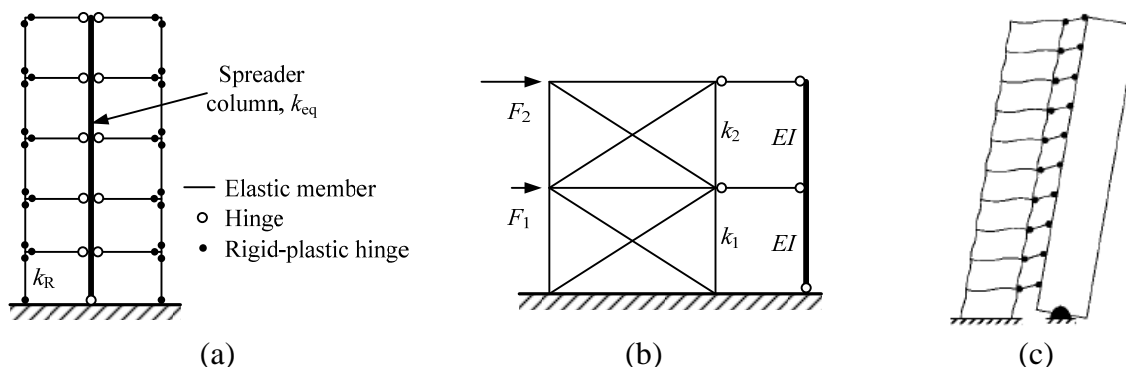


Figure 2 Structural models with pin-supported columns or walls: (a) spreader column by Akiyama (1984) [9]; (b) continuous column by MacRae et al. (2004) [11]; and (c) hinged wall by Alavi et al. (2004) [15]

Energy dissipation capacity is also important for improving the seismic performance of dual systems. Innovative solutions for introducing energy dissipation capacity with walls have been explored for another category of flexible base walls in dual systems, generally referred to as rocking walls. Unlike the above-mentioned pin-supported walls, rocking walls have inherently self-centering capacities. However, they share the same concept in that walls, which play an important role in reducing the damage concentration of a dual system, can be made free of damage even under major earthquakes by releasing the rotational constraint at the base. Precast rocking walls with energy dissipating devices were tested by Holden et al. [16] and later by Restrepo and Rahman [17]. Tapered reinforcing bars that were anchored at the bottom interface and close to the mid-length of the wall were adopted as energy dissipaters in their practice. Ajrab et al. [18] proposed a rocking wall-frame system with supplemental tendon systems. Post-tensioning tendons connecting the top of the rocking walls and the foundation are linked in series with dampers to work as fuses and to provide energy dissipation capacity. Various tendon profiles have been examined. Marriot et al. [19] introduced an experimental study for another energy dissipation solution for rocking walls. Steel dampers and/or viscous dampers are installed at the rocking wall base to dissipate energy when the wall rocks. Toranzo et al. [20] extended the application of rocking walls to confined masonry structures and tested a 3-story structure segment with a confined masonry rocking wall on shaking table. Specially designed steel arms were attached to the surfaces of the wall base to dissipate energy. It should also be noted that several construction projects in the U.S. have been completed where rocking walls are applied. Panian [21] introduced the retrofit of a 6-story reinforced concrete frame with post-tensioned rocking walls. Stevenson [22] introduced a new 4-story office building protected by similar rocking walls.

In the present paper, post-tensioned pin-supported walls are applied to strengthening an 11-story steel reinforced concrete (SRC) frame. Taking advantage of the plan layout of the

existing structure, an alternative energy dissipating solution is proposed. Before going into detail regarding the retrofit project, some basic considerations about pin-supported wall-frame dual systems are introduced below.

2 Pin-supported wall-frame systems

The pin-supported wall-frame system introduced herein is illustrated in Figure 3(a). The pin-supported wall is connected with the frame at each floor level by horizontal connections. Dampers are distributed along the height of the building between the pin-supported wall and the adjacent frame columns. When subjected to lateral earthquake action that is represented by a horizontal arrow with symbol V in Figure 3(b), the structure deforms laterally and the wall rotates around its bottom hinge. The uplift of one side and sinking of the other side of the wall produce vertical displacement between the wall and the adjacent columns. The dampers are expected to dissipate a great portion of the earthquake input energy, taking advantage of this vertical displacement. In Figure 3(b), the dampers are replaced with their forces $F_{D,i}$ acting on the columns and the wall and it is assumed that the force in the two dampers on both sides of the wall at identical level is the same. For the convenience of illustration, the lateral forces that are transmitted between these three parts by horizontal connections are omitted in Figure 3(b) and will be discussed later.

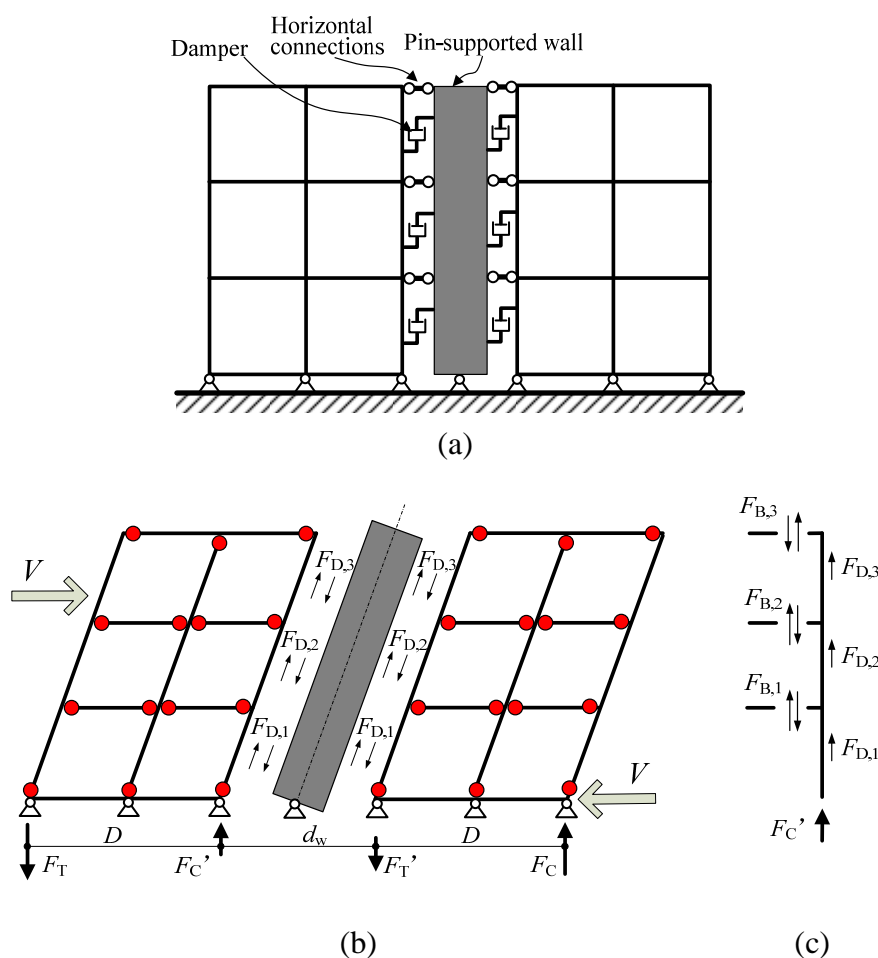


Figure 3 Pin-supported wall-frame system: (a) main components; (b) lateral resistance; and (c) vertical forces in the column connected with pin-supported wall

As a simple example, assuming that all rotations at beam-to-column joints lying at each floor level are identical, that the frames to the right and to the left of the wall are identical and that each beam has a uniform cross-section, the axial force in the two outmost columns due to the earthquake action, V , is identical in absolute value, i.e., $F_T = F_C$, and forms a couple. Likewise, the axial force in the two columns next to the wall, F_C' and F_T' , also forms a couple. Therefore, the moment resistance of the whole system, M_R , can be written as below.

$$M_R = F_C(2D + d_w) - F_C' \cdot d_w \quad (1)$$

where D is the length of each frame part and d_w is the distance between the two columns next to the wall.

Substituting $F_C' = F_C - \sum F_{D,i}$, which can be readily derived from the axial force equilibrium of the column next to the wall (See [Figure 3\(c\)](#)), into [Equation 1](#), it can be rearranged into [Equation 2](#), with which it becomes clear to see that the pin-supported wall produces not only a more uniform story drift distribution, but also some additional moment resistance to the system (i.e., the second term on the right hand side) when working together with dampers.

$$M_R = 2F_C \cdot D + \sum F_{D,i} \cdot d_w \quad (2)$$

The global behavior of such a dual system can be very similar to that with conventional fixed-base shear walls. However, only the translational resistance is retained by the bottom hinges in a pin-supported wall. Moment resistance is released from the bottom of the walls and is distributed along the height of the walls by the use of dampers, which are specifically designed to sustain large plastic deformation and dissipate energy.

Another effect of this configuration of dampers is that the frame columns connected with the dampers must resist the large axial force transmitted from the dampers, e.g., $F_{D,i}$ in [Figure 3\(c\)](#). Column axial force N can then be expressed as [Equation 3](#). Fortunately, as shown in [Figure 3\(c\)](#), $F_{B,i}$ and $F_{D,i}$ tend to act in opposite directions and thus the dampers are not expected to dramatically increase the column axial force.

$$N = G + \sum F_{B,i} + \sum F_{D,i} \quad (3)$$

where G is the axial force due to gravity and $F_{B,i}$ is the shear force in the beam end of the i^{th} floor.

In a wall-frame dual system, walls work as balancers that transfer redundant strength somewhere in the system to where the strength is inadequate. [Figure 4](#) demonstrates a simplified dual system with a pin-supported wall and two single-story subassemblies, which are connected to the pin-supported wall by horizontal links at different levels. In this model, the pin-supported wall provides no additional lateral resistance.

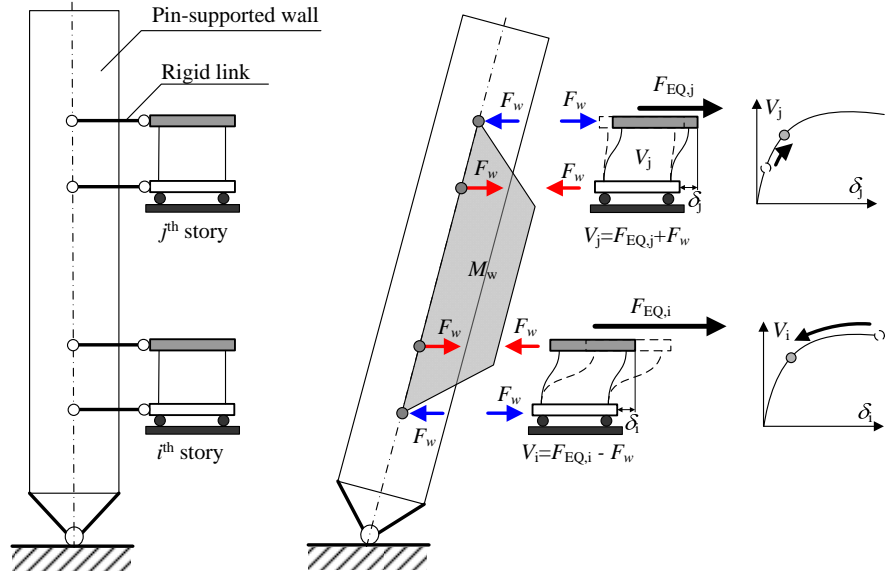


Figure 4 Mechanism of deformation pattern control by pin-supported walls

Assume that the strength of the i^{th} story alone is not adequate to resist the earthquake action $F_{EQ,i}$ and is expected to go deep into the plastic regime and sustain large deformation. With the existence of the pin-supported wall, the lateral drift of this story will be forced to be similar to those of other stories by an additional resisting force of F_w provided by the wall. At the same time, the j^{th} story, where the strength is redundant, must resist an additional force F_w , which is imposed by the wall. Thus, the deformation of this story is increased. In other words, weaker stories are using strength from stronger ones so that they will not fail prematurely. At the same time, the pin-supported wall must sustain the resultant shear force and moment so that this mechanism can be retained even during strong earthquakes.

3 Implementation of pin-supported wall-frame system: the Tokyo Tech G3 Building

A pin-supported wall-frame system has been implemented in the retrofit of an 11-story SRC frame structure, the G3 Building on the Suzukakedai campus of the Tokyo Institute of Technology in Japan [23, 24]. Design of the original SRC frame of the G3 Building began in 1977; construction was completed in 1979. During construction, in 1978, the M7.4 Miyagiken-oki earthquake hit Japan and led to a major revision of the seismic provisions of Japan in 1981 [25]. As concluded by a recent seismic inspection, there was an urgent need to strengthen the G3 Building.

The retrofit plan is depicted in Figure 5. The structural layout of the original frame is feathered with six slots distributed along the perimeter. This makes the attachment of pin-supported walls much easier. Six post-tensioned concrete walls with bottom hinges are installed in the original slots and connected to the existing frame at each floor level by horizontal trusses behind them. Shear-type steel dampers are installed in the gaps between the pin-supported walls and adjacent original columns as well as between the walls and added transverse shear walls at both ends. The main components of the retrofitting plan, as shown in Figure 5, are visible from outside the building so passersby can appreciate the engineering solution.

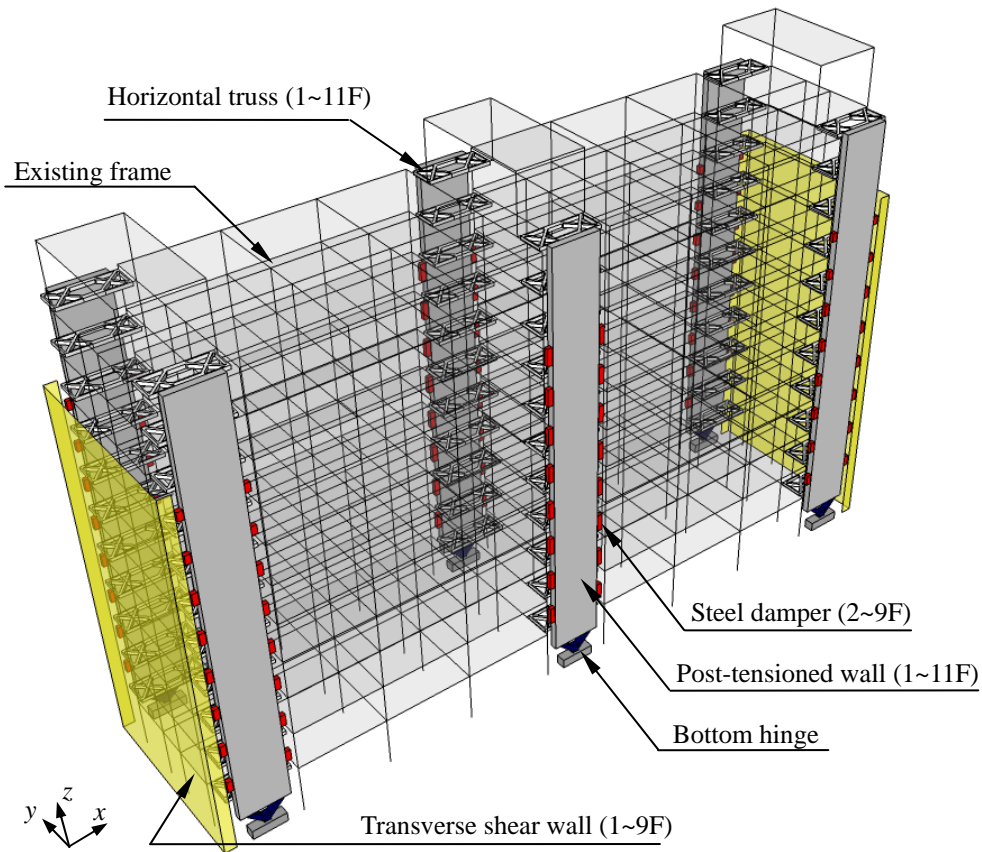


Figure 5 Retrofit plan of G3 Building

3.1 Post-tensioned concrete walls

All six pin-supported walls have identical cross sections of 4300 mm in width and 600 mm in depth, as shown in Figure 6. The total cross-sectional area of the pin-supported walls at each story is about 50% to 61% of that of the original SRC columns from the lower to upper stories. Concrete with 36 MPa nominal compressive strength is used. Each wall is prestressed by six units of post-tensioning tendons. Each unit consists of 30 strands each 12.7 mm in diameter. The initial prestress for each wall is 22500 kN and corresponding control stress is about 68% of the nominal tensile strength of the strand. The resultant effective prestress is expected to be over 18000 kN for each wall. The purpose of prestressing is primarily to prevent cracking and consequent stiffness degradation of the walls under strong earthquakes since the stiffness is believed essential to control the deformation pattern of the structure.

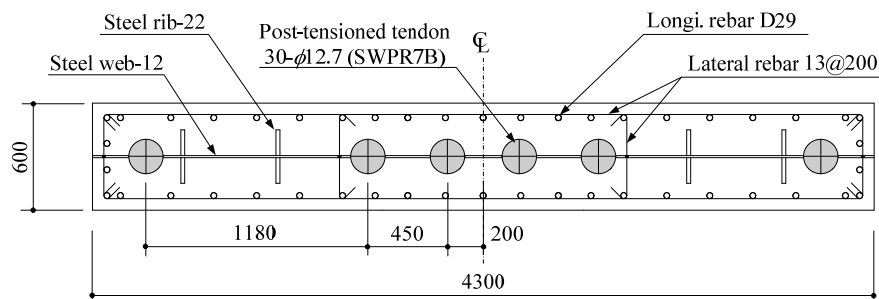


Figure 6 Cross section of post-tensioned wall

3.2 Connections for pin-supported walls

Pin-supported walls are connected to the foundation and the existing frame. The bottom hinge is made of two pairs of steel braces contacting each other through a tooth-like pin bearing. Details and a photo of one of the completed bottom hinges are shown in Figure 7.

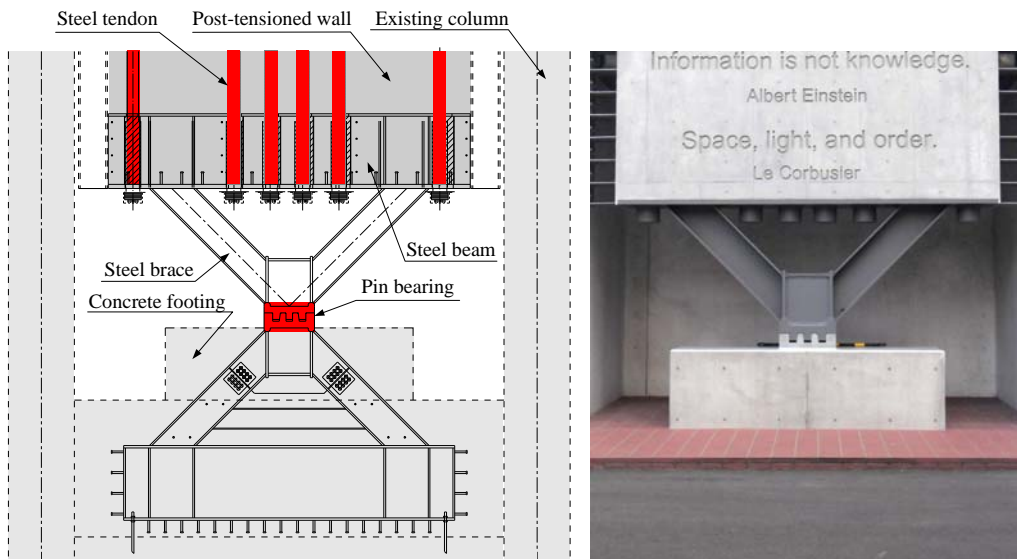


Figure 7 Bottom hinge

The tooth-like pin bearing is made of cast iron NCH490 with a nominal yield strength of no less than 325 MPa. It consists of two separated tooth-shaped pieces (the lower and upper pieces), which interlock with several teeth and a separated stopper in the middle to prevent slip in the out-of-plane direction (Figure 8). The teeth in the lower piece are 20 mm longer than are those in the upper one to create a small gap, and their tips are chamfered to allow for rotation of the upper piece. The shear resistance of a single pair of teeth (i.e., at the critical shear surface in Figure 8) is over 7000 kN, which is about 2.7 times the base shear demand for a pin-supported wall. The shear demand is based on nonlinear time history analysis results with one code-stipulated and two site-specific ground motions.

To avoid uplift of the pin-supported walls due to damper forces, which might lead to dislocation of these walls from the pin bearings, the steel dampers are always arranged on both sides of the walls, even those at both ends of the building, so that the damper forces on both sides of a wall form a force pair and the resultant vertical force on the wall becomes insignificant. Besides, vertical ground motion-induced forces on a pin-supported wall can be resisted by the dampers, the total yield strength of which is more than 5 times the self weight of a pin-supported wall.

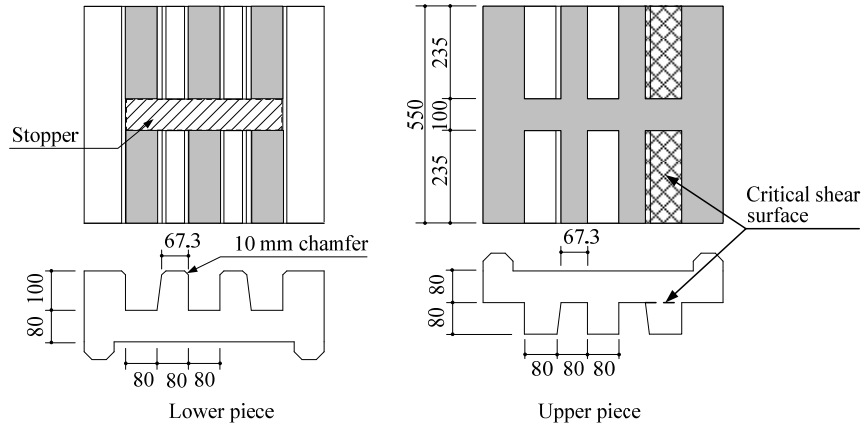


Figure 8 Details of pin bearing

Pin-supported walls are connected to the existing frame mainly by horizontal trusses at each floor level behind them. As Figure 9 shows, the horizontal trusses are firmly anchored to the original beams. Steel shear keys are used to connect the horizontal trusses and pin-supported walls, which impose very small rotational constraints for pin-supported walls. The principal functions of the horizontal trusses are to transmit lateral forces between the pin-supported walls and the original frame and to provide out-of-plane support for the walls.

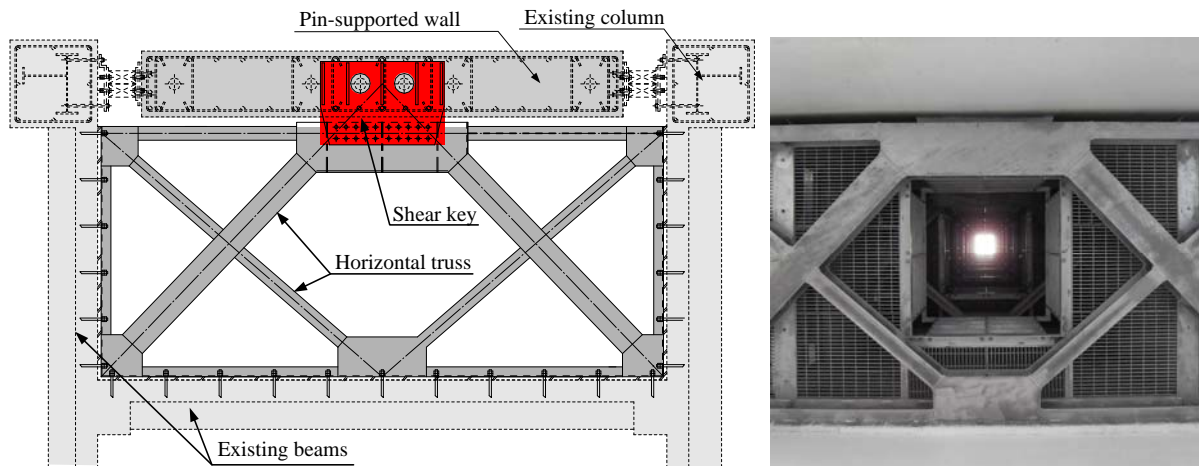


Figure 9 Horizontal truss

3.3 Shear-type steel dampers

Shear-type steel dampers are aligned on both sides of each pin-supported wall. Low yield steel with 130 MPa nominal shear strength is used. Steel webs 6 mm thick, which are stiffened by ribs at 250 mm spacing, function as energy dissipaters. The web height H is 312 mm for all the dampers while the length L varies from 750 mm to 1500 mm (Figure 10(a)). Table 1 lists the web length L of steel dampers in different locations. Figure 10(b) is a photo of an installed steel damper with $L = 1500$ mm. Cyclic loading test of the steel dampers reveals that the nominal shear capacity of the damper can be satisfactorily retained at up to 9% shear strain, which is about 58 times the yield shear strain of the damper [26, 27]. The nominal shear capacity is calculated by multiplying the steel nominal shear strength and the cross-sectional area of the web. A deformed 750 mm steel damper at 9% shear strain and its hysteresis loop is shown in Figure 11. Most earthquake input energy is expected to be dissipated by these steel dampers.

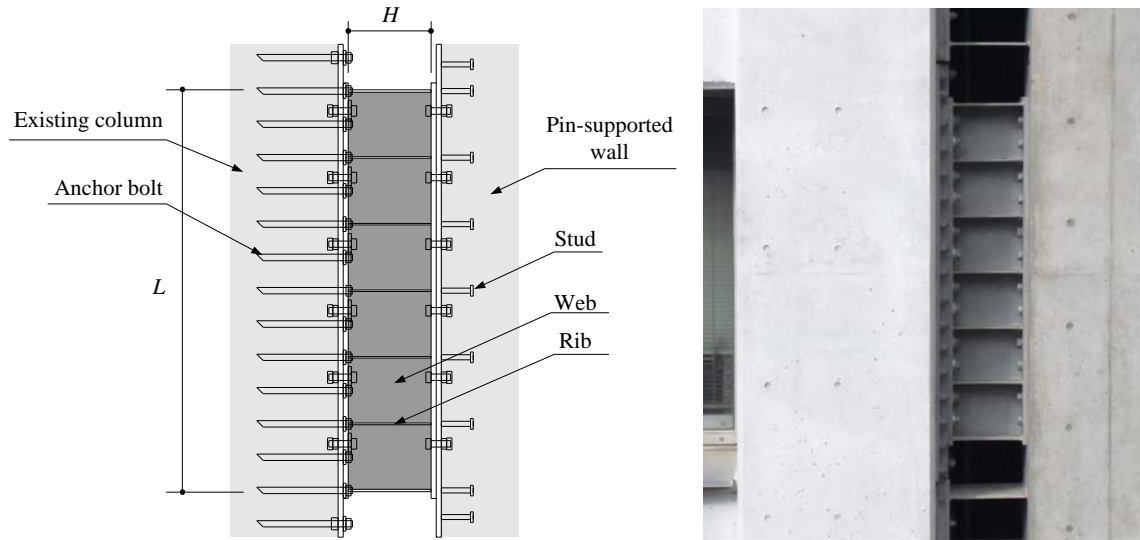


Figure 10 Completed steel damper with $L = 1500$ mm

Table 1 Web length L of steel dampers (Unit: mm)

Story	Central wall	Side wall
8 and 9	1500	750
2~7	1500	1000

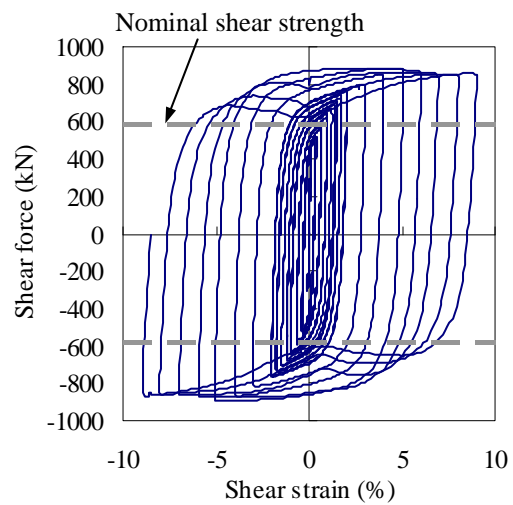


Figure 11 Deformed steel damper and its hysteretic response to cyclic loading ($L = 750$ mm) [26, 27]

4 Seismic performance assessment of the G3 Building

4.1 Numerical model

Dynamic responses of the G3 Building before and after the retrofit to strong earthquakes are evaluated through nonlinear dynamic analysis in ABAQUS 6.8. Due to the symmetry, a half structure along the x -direction (See Figure 5, longitudinal direction) is modeled by a 3-bay SRC plane frame. Nodes sharing the same x (longitudinal) and z (vertical) coordinates in the

three bays are constrained to have the same translational displacement in the x -direction. User-defined material models for steel and concrete fibers are employed in the fiber-based beam element in ABAQUS to model the hysteretic behavior of the SRC members (Figure 12). Shear failure of these members is not modeled. A mass proportional damping model is used and a 2% damping ratio is assigned for the 1st mode. The concrete compressive strength of the existing frame is 20 MPa. The steel yield strength is 394 MPa for the longitudinal reinforcement bars and 358 MPa for the latticed steel reinforcement.

A strength deterioration model is incorporated in the steel fiber to model the degradation of the SRC members under cyclic loading (Figure 13(b)). An ultimate strain for steel fiber ϵ_u is defined as a function of the axial load ratio and volumetric lateral reinforcement ratio of the component. Beyond ϵ_u , the stress-strain envelope drops with a negative stiffness half the Young's modulus of steel, mainly an attempt to avoid numerical difficulty due to sudden loss of strength. The steel yield strength also deteriorates as a function of the ultimate strain, accumulative hysteretic energy dissipation, and maximum strain in the loading history. Detailed descriptions and verifications of this model can be found in Ref [28]. In determining ϵ_u for the original SRC members, a low volumetric lateral reinforcement ratio of 0.2% is assumed to approximately address the fact that these members, which were designed and constructed in the 1970s, generally have inadequate deformability [29].

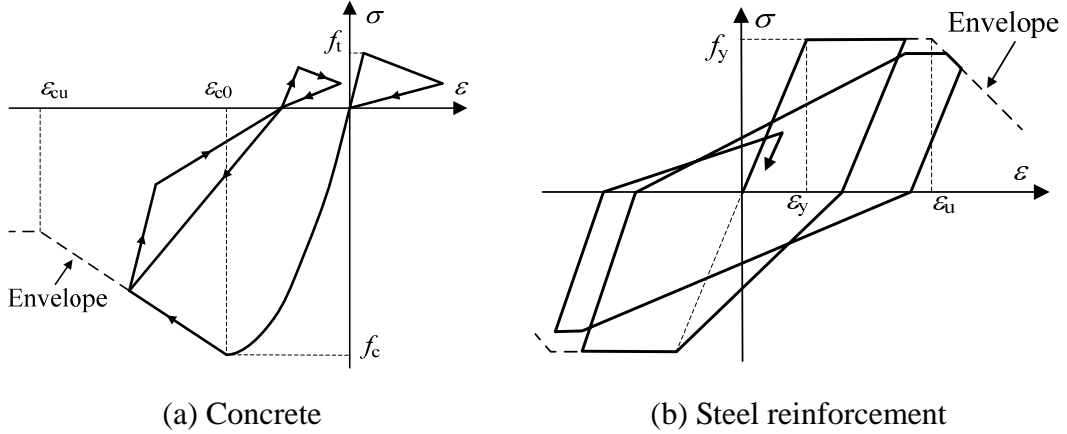


Figure 12 Uniaxial hysteresis of user-defined material models

In modeling the retrofitted building, post-tensioned concrete walls are assumed to remain linear-elastic throughout the analysis and are modeled by beam elements and rigid perpendicular arms. The displacement constraints in Equation 4 are imposed on pin-supported wall nodes at each floor level to model the actions of the horizontal trusses (See Figure 13). The rotational and vertical translational degrees of freedoms are not constrained.

$$x_{w,i} = (x_{R,i} + x_{L,i})/2 \quad (4)$$

where x is the horizontal coordinate of the node. Subscript w denotes nodes on the pin-supported wall while R and L denote nodes of original columns or added transverse walls on the right and left side of pin-supported walls, respectively. Subscript i is the story number.

The steel dampers are modeled by vertical springs that are connected to the ends of the rigid arms reaching from the pin-supported wall and the SRC column, as shown in Figure 13. The hysteretic behavior of the steel dampers is idealized as elastic-perfectly plastic with the nominal yield strength. Neglecting the strain hardening of the steel damper is considered

conservative since both strength and energy dissipation of the dampers will be underestimated. On the other hand, however, the strength demands for the pin-supported walls and energy dissipation demands for the steel dampers might also be underestimated.

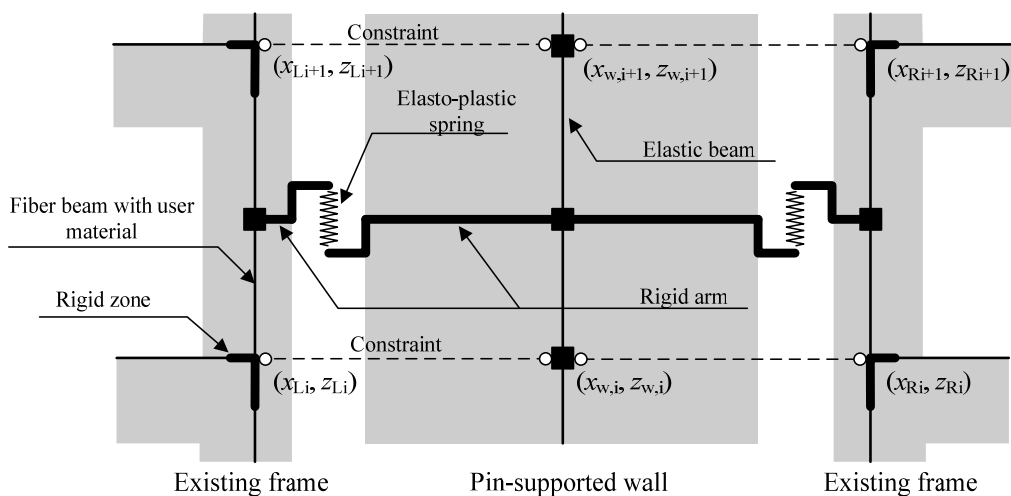


Figure 13 Modeling of pin-supported walls and steel dampers

4.2 Ground motion records

Earthquake ground motion records in the Far-Field Set in [FEMA P695 \[30\]](#) are adopted herein in dynamic analysis while a normalization strategy different from [FEMA P695](#) is used. In [FEMA P695](#), the records are normalized by the geometric mean of the peak ground velocities (PGV) of the two horizontal components. In this study, each record is first rotated to the direction where the maximum PGV occurs. The ground acceleration time history in this direction is then used in the analysis as earthquake input and the corresponding PGV serves as the basis for normalization.

In the following analysis, all records are normalized to $PGV = 50 \text{ cm/s}$, which generally represents the Level II earthquake in Japanese seismic design practice. The velocity spectra of the normalized records are shown in [Figure 14](#).

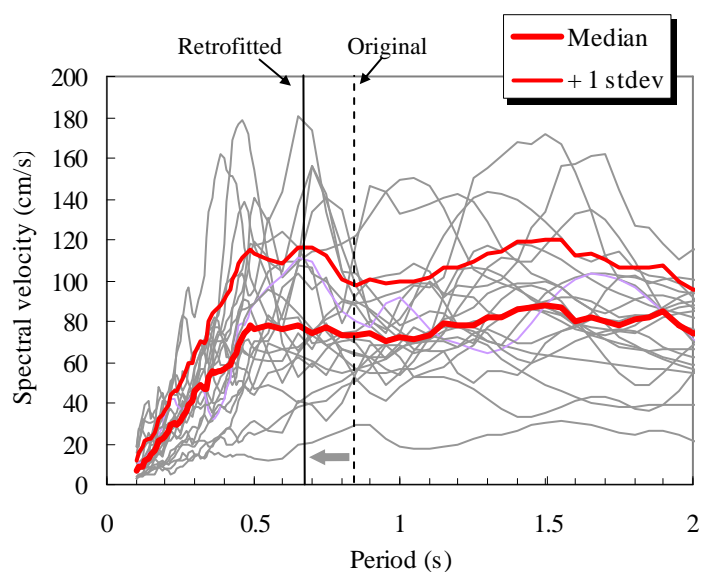


Figure 14 Spectral velocity of the 22 ground motion records normalized to $PGV = 50 \text{ cm/s}$ (5%

damping)

The median and one-standard deviation spectra are also plotted. It can be seen that the median spectral velocity in the period range of 0.5-2.0 s is almost constant around 80 cm/s for the record set. After being retrofitted, the fundamental period of the G3 Building shortens from 0.86 s to 0.68 s. The corresponding median spectral velocity is slightly increased.

5 Results and discussion

5.1 Inter-story drift

Inter-story drift ratio (IDR) is frequently used as a measure of damage in assessing the seismic performance of multi-story building structures. Figure 15 plots IDRs of the G3 Building before and after the retrofit under the normalized ground motions. The median and 84th percentile responses are also plotted. The original structure experiences extremely large IDRs in certain stories under several of the ground motions, indicating collapse at these stories (Figure 15a). In contrast, the distributions of IDRs over the height of the retrofitted building under various ground motion records are much more uniform (Figure 15b).

To better understand the distinct roles of pin-supported walls and steel dampers in the current dual system, seismic responses of an imaginary structure strengthened with pin-supported walls but without steel dampers, denoted as “w/o Damper” hereafter, are assessed. The medians of IDRs of the three structures, denoted as “Existing” (original), “Retrofitted,” and “w/o Damper,” are compared in Figure 16(a). It is obvious that the walls create a much more uniform distribution of IDRs while the dampers further reduce the global deformation of the building. The effectiveness of pin-supported walls in reducing inter-story drift concentration can also be seen in Figure 17, where the inter-story drift concentration is expressed in terms of the drift concentration factor (DCF), as defined in Equation 5.

$$DCF = \frac{\max_i(\text{IDR}_i)}{u_r / H} \quad (5)$$

where u_r is the roof displacement; H is the total height of the structure; and the subscript i is the story number.

DCFs are significantly reduced for many of the ground motions by adding the pin-supported walls. The variance of DCFs under different ground motions also becomes much smaller. This suggests that individual stories in a pin-supported wall-frame system tend to work as a whole to resist earthquake action. The integrity of structures is thus increased and weak story failure can be avoided.

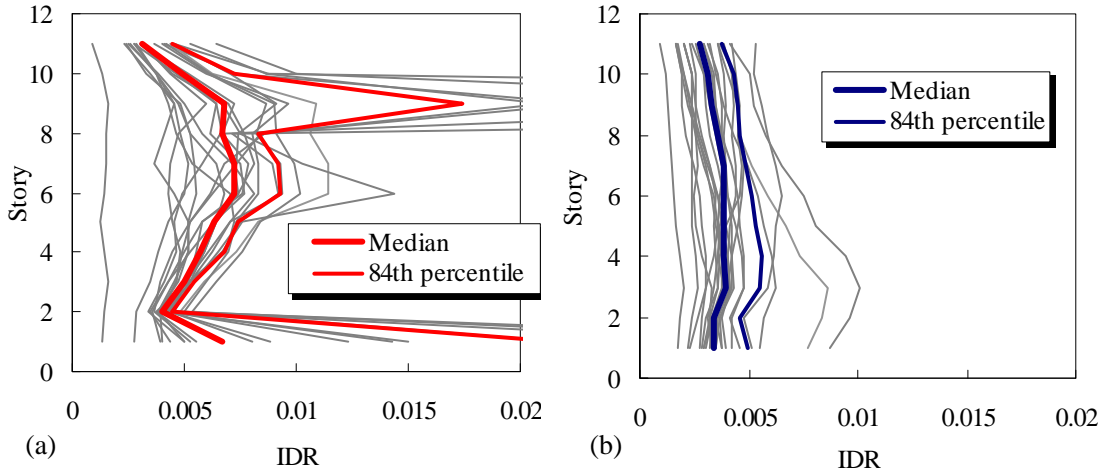


Figure 15 Story drift ratios of G3 Building before and after being retrofitted: (a) existing (original) structure and (b) retrofitted structure

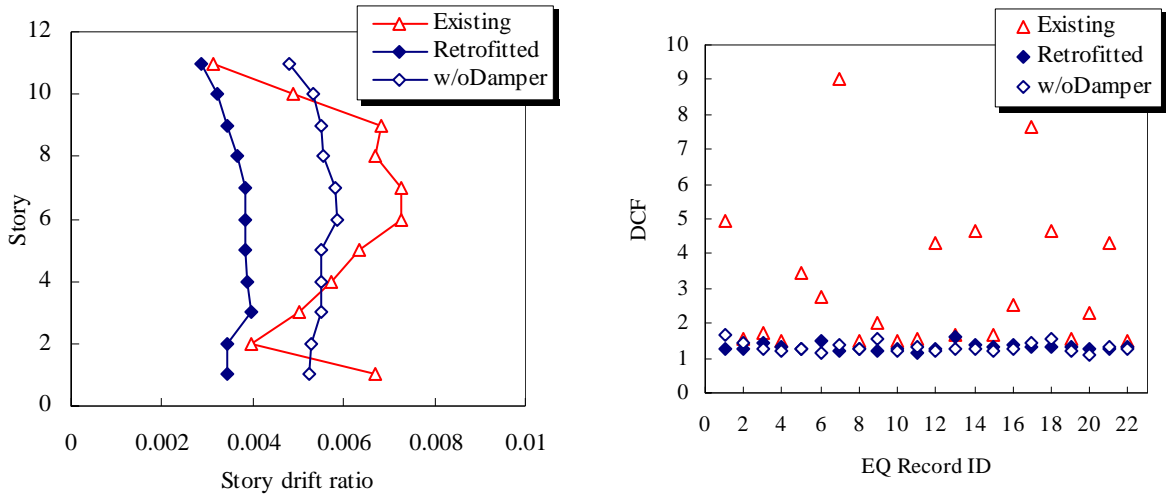


Figure 16 Median IDRs before and after retrofit

Figure 17 Drift concentration factor (DCF) before and after retrofit

5.2 Story shear demand and shear distribution

The shortening of the vibration period because of the retrofit leads to an increase in base shear demand for the building. Figure 18(a) compares the median shear demands of the original and retrofitted structures obtained by linear-elastic time history analysis. The total base shear of the retrofitted building is greater than is that of the original one. This increased part is primarily carried by the pin-supported walls, and the shear demand for the frame before and after the retrofit is almost the same. However, the shear demand distribution for the frame is changed because of interaction with the pin-supported walls. In this specific case, the shear demands for the 2nd and top story are increased while those for the middle stories are reduced. It should be noted that the 2nd and top story of the original structure sustain relatively small deformation in a median sense as compared with other stories (See Figure 16).

Median shear distributions with nonlinear models are shown in Figure 18(b). Different from dual systems with fixed based walls, the pin-supported walls carry a relatively small part of the story shear and most is carried by the frame in the pin-supported wall-frame system.

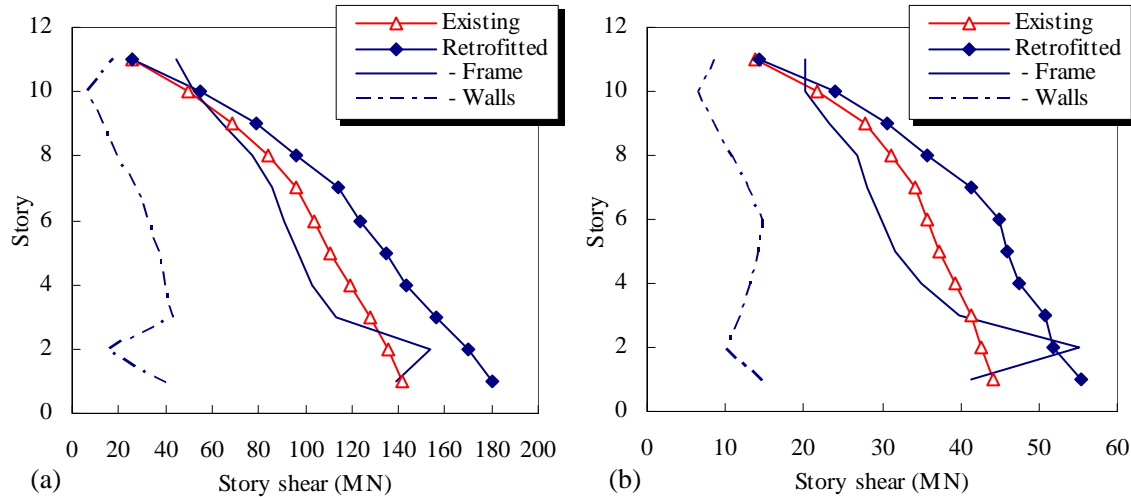


Figure 18 Story shear distributions along the height of the building and among different parts: (a) linear elastic and (b) nonlinear

5.3 Energy dissipation

Pin-supported walls alone do not provide additional energy dissipation capacity. They only help in making better use of the seismic capacities of other structural components by controlling the deformation pattern. Taking advantage of the controlled deformation pattern, steel dampers installed between pin-supported walls and the rest of the structure work well to concentrate energy dissipation (or, in other words, to concentrate the damage). Before the retrofit, most damage and energy dissipation occur in the frame columns, which is undesirable for frame structures (Figure 19a). With the assistance of pin-supported walls (i.e., in the “w/o Damper” model), the average percentage of energy dissipated in beams increases slightly and its coefficient of variance is reduced (Figure 19b). After full retrofitting, energy dissipation in the frame is significantly reduced. On average, most hysteretic energy dissipation goes into the steel dampers (Figure 19c).

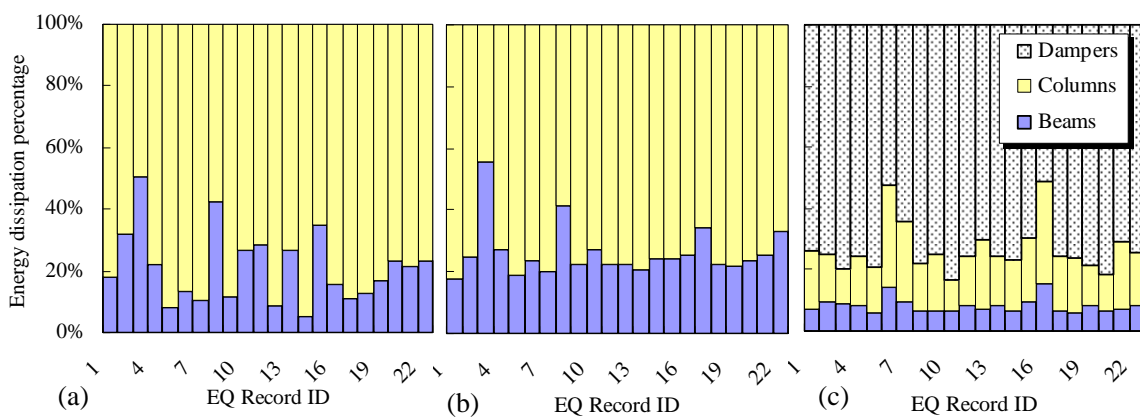


Figure 19 Distribution of energy dissipation among different types of components: (a) existing (original) structure; (b) retrofitted structure without dampers; and (c) retrofitted structure

The distribution of hysteretic energy dissipated by the steel dampers at different story levels is shown in Figure 20. It can be seen that the energy dissipation decreases rapidly from the lower to upper stories, and the steel dampers at the 2nd story become the most vulnerable.

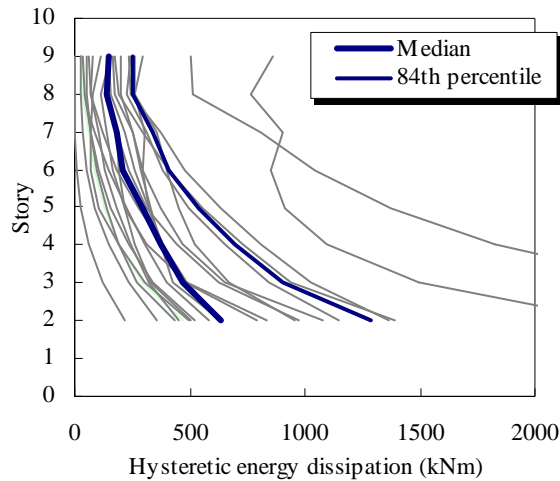
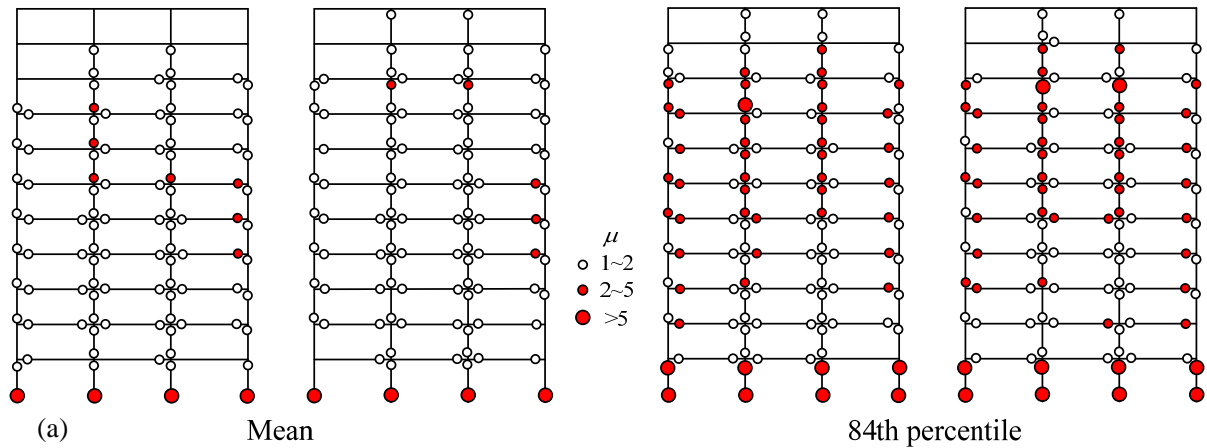


Figure 20 Distribution of hysteretic energy dissipated by steel dampers

5.3 Damage to the frame

As most earthquake input energy is dissipated by the steel dampers, damage to the frame is expected to be significantly reduced. Figure 21 illustrates the median and 84th percentile ductility factors μ at the beam and column ends. Ductility factor μ is defined as the ratio of maximum and yield curvature of the reinforced concrete section. For the convenience of demonstration, ductilities fall into three categories, representing “minor damage” ($\mu = 1\sim 2$), “moderate damage” ($\mu = 2\sim 5$), and “severe damage” ($\mu > 5$). Corresponding to the energy dissipation results, damage to the concrete members in the retrofitted structure is obviously reduced. The importance of the steel dampers in reducing damage to the frame can also be seen by comparing the ductility results of the retrofitted structure and the “w/o Damper” structure.



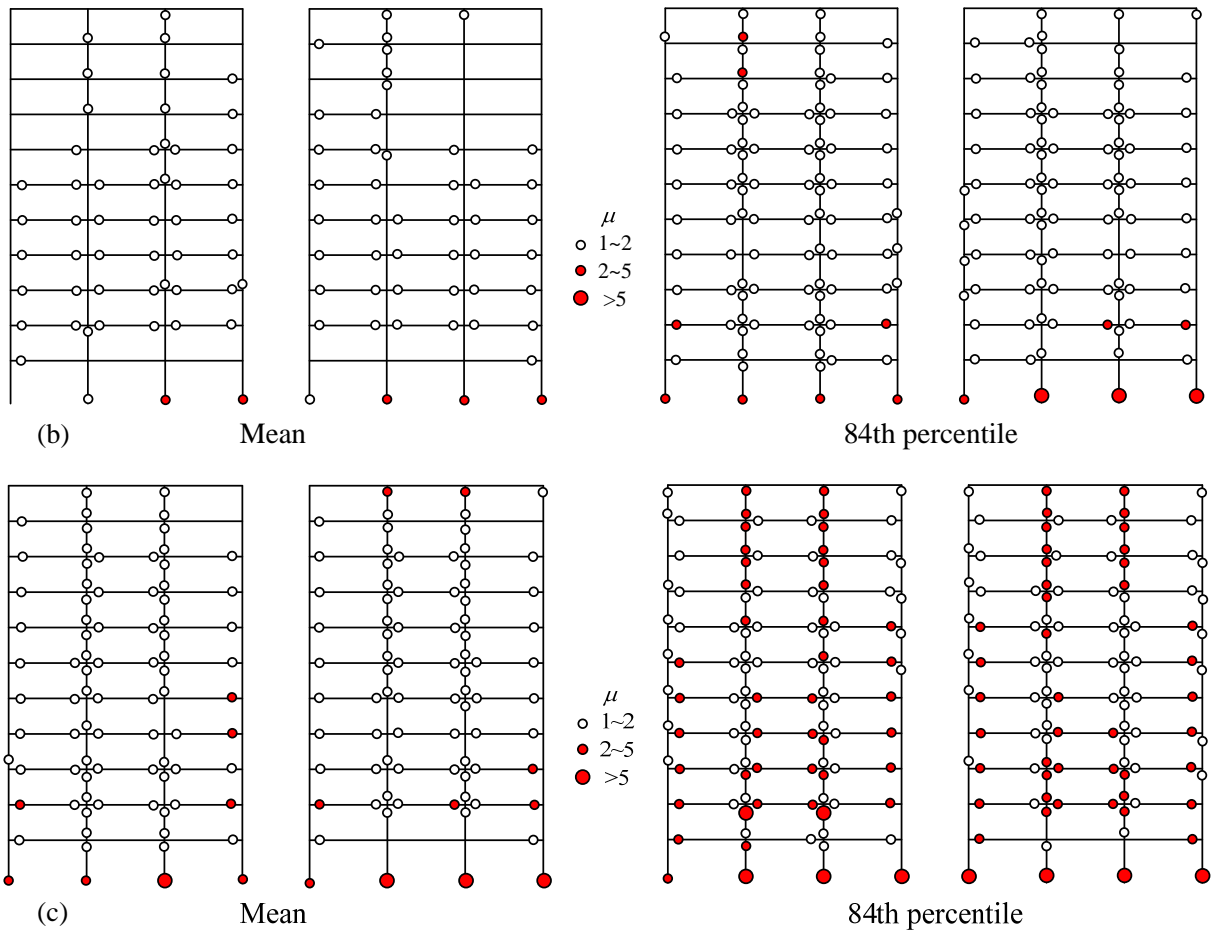


Figure 21 Ductility distributions of the outermost frame: (a) existing (original) structure; (b) retrofitted structure; and (c) retrofitted structure without dampers

As mentioned above, the existence of steel dampers may impose significant axial force on the columns next to the pin-supported walls. Figure 22 compares the median compressive and tensile force ratio of such a column before and after the retrofit. The column is next to the pin-supported wall in the middle of the building. The compressive force ratio is defined as the ratio of maximum compressive force to the compressive strength $N_{cu} = f_c A_c + \sum f_y A_s$, where f_c is the concrete compressive strength, A_c the concrete cross-sectional area, f_y the steel yield strength, and A_s the steel cross-sectional area. Similarly, the tensile force ratio is defined as the ratio of maximum tensile force to the tensile strength N_{tu} , which is simply taken as the yield strength of all its reinforcement, i.e., $N_{tu} = \sum f_y A_s$.

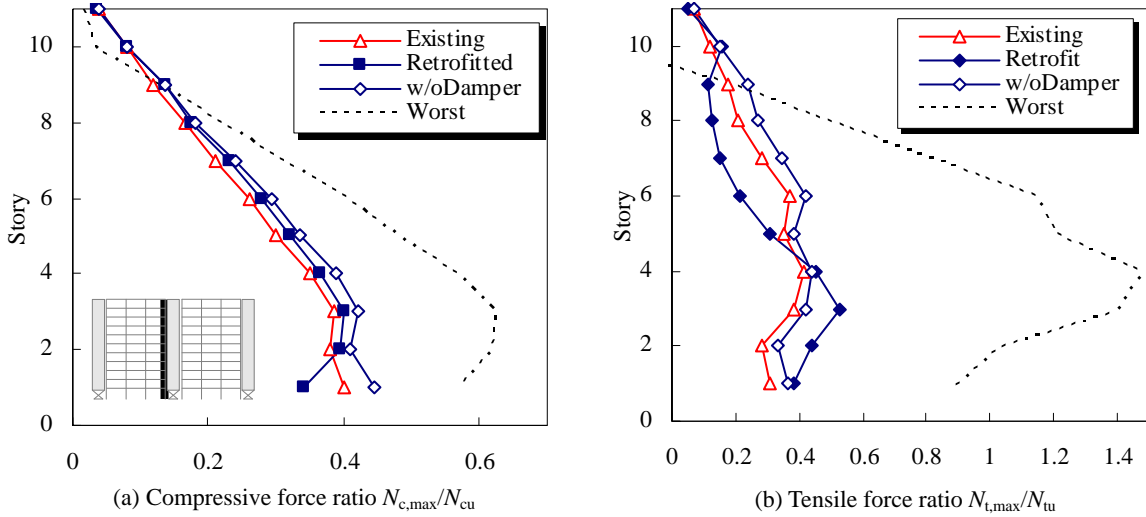


Figure 22 Median axial force ratios of columns

The dotted lines in Figure 22 represent the worst situation in which all dampers along the column yield in the same direction and the column axial force comes only from the damper forces and the gravity load. That is, $N_t = \sum F_{Dy} - G$ and $N_c = \sum F_{Dy} + G$, where F_{Dy} is the damper yield strength and G is the axial force due to gravity. In this case, the column tension may reach its tensile strength N_{tu} and lead to tensile failure of the column. As shown in Figure 22, the maximum axial force in the column is, however, not that dramatically changed before and after the retrofit because the beams will also impose axial forces on the columns as described earlier in Figure 3(c). Nevertheless, Figure 22(b) reveals that the column may sustain considerable tension in both the original and retrofitted structures and the maximum tension is increased in the lower stories after the retrofit. Although it does not exceed the tensile strength, this tension will degrade the flexural and shear strengths and might lead to undesired shear failure of the column at the lower stories. Note that shear failure of the SRC members is not taken into account in the current analysis. The vulnerability of the building would have been underestimated, especially for the unretrofitted structure, which is more sensitive to local failure than is the retrofitted one.

6 Conclusions

The retrofit of an 11-story steel reinforced concrete frame using post-tensioned pin-supported walls is introduced. An alternative arrangement of energy dissipating devices is adopted in which shear-type steel dampers are distributed along the height of pin-supported walls.

Linear-elastic and nonlinear dynamic analysis is carried out to compare the seismic performance of the building before and after the retrofit. The results show that:

- (1) Pin-supported walls are capable of creating a much more uniform distribution of story drift and thus avoiding undesirable weak story failure of moment-resisting frames.
- (2) Shear demand of the frame is increased at the floors sustaining relatively small deformation, and is decreased at other floors, which are likely to suffer excessive plastic

deformation.

(3) Taking advantage of the well-controlled deformation pattern, steel dampers along the sides of the pin-supported walls are effective in concentrating energy dissipation.

(4) With the protection of the pin-supported walls and steel dampers, damage to the frame can be significantly reduced. However, some local parts of the frame, such as the columns connected with the steel dampers, might be subjected to more severe loading conditions.

The retrofit project provides an alternative solution for strengthening moment-resistant frames. Although equipped with several specifically designed devices, e.g., the steel dampers and the bottom hinges, the introduced retrofit plan turned out to be more economical than other conventional retrofit plans for the G3 Building, such as strengthening individual columns. To make it more economically feasible, most of the construction is done from outside the building and occupancy of the building need not be suspended during the retrofit.

Acknowledgments

The authors acknowledge the contributions of Prof. S. Midorikawa and Prof. H. Yamanaka of the Structural Engineering Research Center of Tokyo Institute of Technology to the retrofit design of the G3 Building for conducting a seismic hazard analysis of the specific site of G3 Building and providing ground motion time histories for the retrofit design.

This study is partly sponsored by the Japan Science and Technology Agency (JST) and the National Natural Science Foundation of China (NSFC) under the Strategic Japanese-Chinese Cooperative Program on “Science and Technology (S&T) for Environmental Conservation and Construction of a Society with Less Environmental Burden.” The research field of the program is “Evaluation and mitigation of environmental impacts of earthquake and typhoon disaster on urban areas and infrastructures.” Their financial support is highly appreciated.

References

1. Villaverde R. Explanation for the numerous upper floor collapses during the 1985 Mexico City earthquake. *Earthquake Engineering & Structural Dynamics*, 1991, 20(3): 223-241.
2. AIJ. Report on the Hanshin-Awaji earthquake disaster-Building series Volume 1: Structural damage to reinforced concrete building. Architectural Institute of Japan (AIJ), 1997 (in Japanese).
3. Civil and Structural Groups of Tsinghua University, Xinan Jiaotong University, and Beijing Jiaotong University. Analysis on seismic damage of buildings in the Wenchuan earthquake. *Journal of Building Structures*, 2008, 29(4): 1-9 (in Chinese).
4. AIJ. Preliminary reconnaissance report of the 2011 Tohoku-Chiho Taiheiyo-Oki earthquake. Architectural Institute of Japan (AIJ), Tokyo, 2011: 105-111 (in Japanese).
5. Paulay T, Priestley M J N. Seismic design of reinforced concrete and masonry buildings. New York: John Wiley & Sons, Inc. 1992: 210-240.
6. SNZ. Concrete structures standard (NZS 3101.1). Standards New Zealand, Wellington, New Zealand, 2004.
7. ACI 318M-05. Building code requirements for structural concrete and commentary. Farmington Hills, Michigan, US: American Concrete Institute, 2005.

8. GB50011-2001. Code for seismic design of buildings. Ministry of Construction of China, Beijing, 2001.
9. Akiyama H, Takahashi M. Ds-values for damage-dispersing type multi-story frames. *Journal of Structural and Construction Engineering, Transaction of AIJ*. 341, 1984: 54-61 (in Japanese).
10. Akiyama H, Takahashi M. Generalization of damage-dispersing type multi-story frames. *Journal of Structural and Construction Engineering, Transaction of AIJ*. 365, 1986: 20-27 (in Japanese).
11. MacRae G A, Kimura Y, Roeder C. Effect of column stiffness on braced frame seismic behavior. *Journal of Structural Engineering, ASCE*, 2004, 130(3): 381-391.
12. Ji X D, Kato M, Wang T, et al. Effect of gravity columns on mitigation of drift concentration for braced frames. *Journal of Constructional Steel Research*, 2009, 65(12): 2148-2156.
13. Tagawa H. Towards an understanding of seismic response of 3D structures - stability & reliability. Doctoral thesis, Washington: University of Washington, 2005.
14. Paulay T, Priestley M J N. *Seismic design of reinforced concrete and masonry buildings*. New York: John Wiley & Sons, Inc. 1992: 500-516.
15. Alavi B, Krawinkler H. Strengthening of moment-resisting frame structures against near-fault ground motion effects. *Earthquake Engineering and Structural Dynamics*, 33(6), 2004: 707-720.
16. Holden T, Restrepo J I, Mander, J B. Seismic performance of precast reinforced and prestressed concrete walls. *Journal of Structural Engineering, ASCE*, 129(3), 2003: 286-296.
17. Restrepo J I, Rahman A. Seismic performance of self-centering structural walls incorporating energy dissipators," *Journal of Structural Engineering, ASCE*, 133(11), 2007: 1560-1570.
18. Ajrab J J, Gokhan P, Mander J B. Rocking wall-frame structures with supplemental tendon systems. *Journal of Structural Engineering, ASCE*, 2004, 130(6): 895-903.
19. Marriott D S, Pampanin D B, Palermo A. Dynamic testing of precast, post-tensioned rocking wall systems with alternative dissipating solutions. *Bulletin of the New Zealand Society for Earthquake Engineering*, 2008, 41(2): 90-103.
20. Toranzo L, Restrepo J I, Mander J B, Carr A J. (2009). Shake-Table Tests of Confined-Masonry Rocking Walls with Supplementary Hysteretic Damping. *Journal of Earthquake Engineering*, 13(6), 2009: 882-898.
21. Panian L, Steyer M, Tipping S. An innovative approach to earthquake safety and concrete construction in buildings. *Journal of the Post-Tensioning Institute*, 2007, 5(1): 7-16.
22. Stevenson M, Panian L, Korolyk M, et al. Post-tensioned concrete walls and frames for seismic-resistance - a case study of the David Brower Center. *Proc. the SEAOC Annual Convention, Hawaii, US*, 2008.
23. Wada A, Qu Z, Ito H, Motoyui S, Sakata H, Kasai K, Seismic retrofit using rocking walls and steel dampers. *Proc. ATC/SEI Conference on Improving the Seismic Performance of Existing Buildings and Other Structures, San Francisco, CA, U.S., Dec. 2009*.
24. Qu Z, Motoyui, S, Sakata H, Kishiki S, Wada A, Seismic retrofit of existing RC building with rocking walls and steel dampers. *Proc. 13th Japan Earthquake Engineering Symposium, Tsukuba, Japan, Nov. 2010* (in Japanese).
25. Aoyama H. Outline of earthquake provisions in the recently revised Japanese building code. *Bulletin of the New Zealand National Society for Earthquake Engineering*, 1981, 14(2), 63-80.
26. Wada A, Uchiyama Y, Motoyui S, et al. Seismic retrofit of existing RC building with rocking wall-Part 1: Retrofit plan and steel damper experiment. *Summaries of technical papers of annual meeting, Architectural Institute of Japan*, 2010, C-2: 623-624 (in Japanese).

27. Uchiyama Y. Seismic retrofit of existing RC building with rocking wall. Master thesis, Tokyo: Tokyo Institute of Technology, 2009 (in Japanese).
28. Qu Z, Ye LP, Strength deterioration model based on effective hysteretic energy dissipation for RC members under cyclic loading. Proc.7th Intl. Conf. on Urban Earthquake Eng. (7CUEE) & 5th Intl. Conf. on Earthquake Eng. (5ICEE), Tokyo, Japan, 2010: 851-856.
29. Architectural Institute of Japan. Recommendation to RC structural design after Hanshin-Awaji earthquake disaster-Cause of particularly noticed damages and corresponding RC structural design details. 1998 (in Japanese).
30. FEMA P695. Quantification of building seismic performance factors. Federal Emergency Management Agency, Washington, D.C., 2009.